2014

Memory accumulation mechanisms in human cortex are independent of motor intentions

Carlo Sestieri
Gabriele d'Annunzio

Annalisa Tosoni
Gabriele d'Annunzio

Valeria Mignogna
Gabriele d'Annunzio

Mark P. McAvoy
Washington University School of Medicine in St. Louis

Gordon L. Shulman
Washington University School of Medicine in St. Louis

See next page for additional authors

Follow this and additional works at: http://digitalcommons.wustl.edu/open_access_pubs

Recommended Citation

Sestieri, Carlo; Tosoni, Annalisa; Mignogna, Valeria; McAvoy, Mark P.; Shulman, Gordon L.; Corbetta, Maurizio; and Romani, Gian Luca ,"Memory accumulation mechanisms in human cortex are independent of motor intentions." The Journal of Neuroscience.34,20. 6993-7006. (2014).
http://digitalcommons.wustl.edu/open_access_pubs/2920

Authors

Carlo Sestieri, Annalisa Tosoni, Valeria Mignogna, Mark P. McAvoy, Gordon L. Shulman, Maurizio Corbetta, and Gian Luca Romani

Behavioral/Cognitive

Memory Accumulation Mechanisms in Human Cortex Are Independent of Motor Intentions

Carlo Sestieri,[1,2] **Annalisa Tosoni,**[1,2] **Valeria Mignogna,**[1,2] **Mark P. McAvoy,**[3] **Gordon L. Shulman,**[4] **Maurizio Corbetta,**[3,4,5] and **Gian Luca Romani**[1,2]

[1]Department of Neuroscience and Imaging, Gabriele d'Annunzio University, 66013 Chieti, Italy, [2]Institute for Advanced Biomedical Technologies, Gabriele d'Annunzio University Foundation, 66013 Chieti, Italy, and Departments of [3]Radiology, [4]Neurology, and [5]Anatomy and Neurobiology, Washington University School of Medicine, St. Louis, Missouri 63110

Previous studies on perceptual decision-making have often emphasized a tight link between decisions and motor intentions. Human decisions, however, also depend on memories or experiences that are not closely tied to specific motor responses. Recent neuroimaging findings have suggested that, during episodic retrieval, parietal activity reflects the accumulation of evidence for memory decisions. It is currently unknown, however, whether these evidence accumulation signals are functionally linked to signals for motor intentions coded in frontoparietal regions and whether activity in the putative memory accumulator tracks the amount of evidence for only previous experience, as reflected in "old" reports, or for both old and new decisions, as reflected in the accuracy of memory judgments. Here, human participants used saccadic-eye and hand-pointing movements to report recognition judgments on pictures defined by different degrees of evidence for old or new decisions. A set of cortical regions, including the middle intraparietal sulcus, showed a monotonic variation of the fMRI BOLD signal that scaled with perceived memory strength (older > newer), compatible with an asymmetrical memory accumulator. Another set, including the hippocampus and the angular gyrus, showed a nonmonotonic response profile tracking memory accuracy (higher > lower evidence), compatible with a symmetrical accumulator. In contrast, eye and hand effector-specific regions in frontoparietal cortex tracked motor intentions but were not modulated by the amount of evidence for the effector outcome. We conclude that item recognition decisions are supported by a combination of symmetrical and asymmetrical accumulation signals largely segregated from motor intentions.

Key words: decision-making; diffusion models; effector specificity; episodic memory; fMRI; parietal lobe

Introduction

In perceptual decision-making, sensory inputs provide information for appropriate action selection. Landmark animal studies (Gold and Shadlen, 2007) have demonstrated that the activity of oculomotor neurons in the lateral intraparietal (LIP) area reflects the accumulation of evidence for perceptual decisions that are reported through eye movements. Because this ramp-like activity was highly consistent with the predictions of drift diffusion models (DDMs) (Ratcliff and McKoon, 2008), it allowed to establish an important link between neurobiology and psychology of decision-making. These findings also represent the basis for an intentional framework for decision-making (Shadlen et al., 2008), according to which decisions are inseparable from the actions used to report them. Human studies have further shown

that perceptual decision signals can be observed in motor regions if sensorimotor associations are explicitly provided (Tosoni et al., 2008; Donner et al., 2009; Gould et al., 2012). Human decisions, however, also frequently rely on episodic memory, such as when we decide to greet people we recognize. Interestingly, diffusion models were originally developed in the context of episodic memory, describing retrieval as a process of evidence accumulation about the relatedness between probes and items in the memory set (Ratcliff, 1978). Recently, moreover, the mnemonic accumulator hypothesis (Wagner et al., 2005; Donaldson et al., 2010; Huijbers et al., 2010) has drawn an explicit analogy between signals for perceptual decision in monkey LIP and fMRI activity observed in human posterior parietal cortex (PPC) during memory retrieval.

Here we examine three outstanding issues concerning the relationship between memory retrieval and decision-making. First, it is unclear whether BOLD activity in PPC during item recognition tracks evidence for both "old" and "new" decisions (i.e., a symmetrical organization consistent with evidence accumulation during perceptual decisions) or only for old decisions (i.e., an asymmetrical organization consistent with a relatedness signal) (Daselaar et al., 2006; Cabeza et al., 2008). Second, it is not clear whether memory accumulator signals can be found in effector-specific regions, as predicted by the intentional framework.

Third, given the heterogeneity of the memory retrieval effects described in PPC (Nelson et al., 2010; Sestieri et al., 2011; Hutchinson et al., 2014), the topography of the putative mnemonic accumulator is still unclear.

To address these issues, here we designed a picture recognition fMRI paradigm involving a parametric manipulation of the amount of evidence favoring old versus new decisions and an across-subject manipulation of the association between the decision (old, new) and the motor effector (eye, hand) used to report it (eye for old decisions, hand for new decisions and vice versa). Based on previous results (Tosoni et al., 2008), we predicted that activity in regions involved in evidence accumulation should positively scale with the amount of memory evidence, before movement execution. Under these assumptions, we used the between-group manipulation of the decision-response mapping to test the relationship between evidence modulation and movement specificity and the parametric manipulation of memory evidence to test whether the putative memory accumulator was organized symmetrically or asymmetrically with respect to old and new decisions.

Materials and Methods
Subjects
Participants gave informed consent in accordance with guidelines set by the Human Studies Committee of G. D'Annunzio Chieti University. Fifteen right-handed subjects (9 males, mean age 30 ± 5 years) participated in the psychophysical experiment, consisting of an encoding and a retrieval session. A different group of 24 right-handed subjects (11 males, mean age 25 ± 3 years) participated in the fMRI experiment. The fMRI experiment involved three sessions in the following order: (1) a localizer session (fMRI) for localizing frontoparietal effector-specific (hand, eye) regions; (2) a memory encoding session (behavioral); and (3) a memory retrieval session (fMRI). The interval between the encoding and the retrieval sessions was ~24 h.

Stimuli
Stimuli consisted of 256 × 256 pixel color photographs depicting indoor and outdoor scenes, selected from a large database (Konkle et al., 2010; http://cvcl.mit.edu/MM). A total of 434 (14 for practice, 420 for the experiment) images were used in the psychophysical experiment. A total of 484 images (64 for practice, 420 for the experiment) were used in the fMRI experiment. The images used in the two experiments were largely overlapping. Few changes were made to exclude those images associated with inconsistent encoding judgments across subjects in the psychophysical experiment. Visual stimuli were presented using E-Prime 1.1 software (Psychology Software Tools).

Apparatus
Behavioral. In the psychophysical experiment, images were presented on a 17′ LCD computer monitor (1024 × 768 pixels, 60 Hz refresh rate) at a distance of 60 cm. Participants responded using a Lumina RB-830 Response Pad. The encoding session of the fMRI experiment was performed inside a mock scanner. Images were projected onto a screen positioned at the back of the scanner via a LCD projector and visible to subjects through a mirror attached over the subject's head. Subjects responded using a Cedrus RB-830 USB Response Pad.

fMRI. In the localizer and the fMRI retrieval session, visual stimuli were projected on a screen located at the head of the magnet bore via a LCD projector and viewed through a mirror attached to the head coil. Subjects wore MRI-compatible earphones and responded using a Cedrus Lumina LU400 fiber optic Response Pad.

Psychophysical experiment
Manipulation of memory evidence. The psychophysical experiment tested whether the manipulation of memory evidence during item recognition selectively affected the rate of evidence accumulation (i.e., drift rate parameter) of the diffusion model. Notably, this was an essential prerequi-

site for running the fMRI experiment. DDMs depict decisions as a diffusion process in which a decision variable gradually drifts toward a bound indicating one of two choices (Smith and Ratcliff, 2004). The model decomposes accuracy and response times into processing components reflecting the rate of evidence accumulation (drift rate), the starting point of the diffusion process, the distance between the starting point and the decision bounds. Another component includes nondecision processes (stimulus encoding and response execution). In the context of old/new decisions (Ratcliff, 1978; Ratcliff et al., 2004), subjective memory strength is thought to be determined by the quality of evidence in the stimulus and thus by the speed (drift rate) of evidence accumulation. In the present study, the amount of evidence favoring old decisions was manipulated by varying the "encoding strength," based on the rationale that the higher number of times an item is repeated during encoding the better its memory representation and thus the match with the corresponding probe at retrieval (Criss et al., 2013). The amount of evidence favoring new decisions was instead manipulated by varying the similarity between old and new images (Fig. 1A). According to the Ratcliff diffusion model (Ratcliff and McKoon, 2008), the drift rate in the diffusion process is equal to a relatedness value, which corresponds to the number of features shared by the probe and the items present in the memory set, and it has been demonstrated that semantic, visual, and phonemic similarities between probe and memory items affect recognition performance (for review, see Ratcliff, 1978). On this basis, we predicted that the higher is the degree of relatedness between retrieval lures and encoded items, the lower the evidence for a new decision. To avoid potential confusion, from here on the term "memory status" will be used to indicate whether an item is objectively old or new, "memory evidence" to indicate the quality of the stimulus favoring old/new decisions, "memory judgment" or "memory decision" to indicate the subjective outcome of the decision process, and "response" to indicate the movement used to report the decision.

Encoding. At encoding, subjects made indoor/outdoor decisions on visually presented images depicting scenes from different categories. Images from 60 categories (30 indoor and 30 outdoor) were presented, each comprising 4 different stimuli, resulting in a total of 240 images. The 4 stimuli in each category were repeated at different frequencies: two images were presented once ["1×" and encoding only ("EO") images], one was presented three times ("3×") and one was presented five times ("5×"). A total of 15 blocks, each including four 1×, four EO, 12 3×, and 20 5× stimuli, were presented. Each trial started with a 500 ms warning red fixation cross on a gray background, followed by image presentation for 1 s. Presentation time was fixed to keep encoding time constant. The image was followed by a 1 s blue fixation cross. Subjects had 2 s from image onset to answer (image + blue cross) by pressing one of two keys of a response pad located under their right hand. A 1 s black fixation cross preceded the next trial. The order of trials was randomized and the judgment-response mapping was counterbalanced across subjects.

Retrieval. Approximately 24 h later, subjects made item recognition decisions on old and new pictures. Old items (N = 180) included the whole set of 1×, 3×, and 5× images presented at encoding while EO images were not presented. Three types of new items (N = 180) were presented, characterized by a decreasing evidence level toward new decisions: images belonging to 60 new categories, which were therefore unrelated ("U") to old images, images belonging to the same 60 encoding categories (semantically related, "SR"), and images belonging to the same categories and also physically similar to EO images ("SPR"). A total of 12 blocks, each including 30 trials, 5 for each of the six retrieval stimulus types, were presented. Each trial started with a 500 ms warning red cross on a gray background, followed by the presentation of the image for 1 s. The image was followed by a 2 s blue fixation cross. Subjects had 3 s from image onset to answer by pressing one of two keys of a response pad located under their right hand. A 1 s black fixation cross preceded the next trial. The order of trials was randomized and the judgment-response mapping was counterbalanced across subjects.

fMRI experiment
The memory paradigm (Fig. 1B) was similar to the one used in the psychophysical experiment, with the introduction of few important
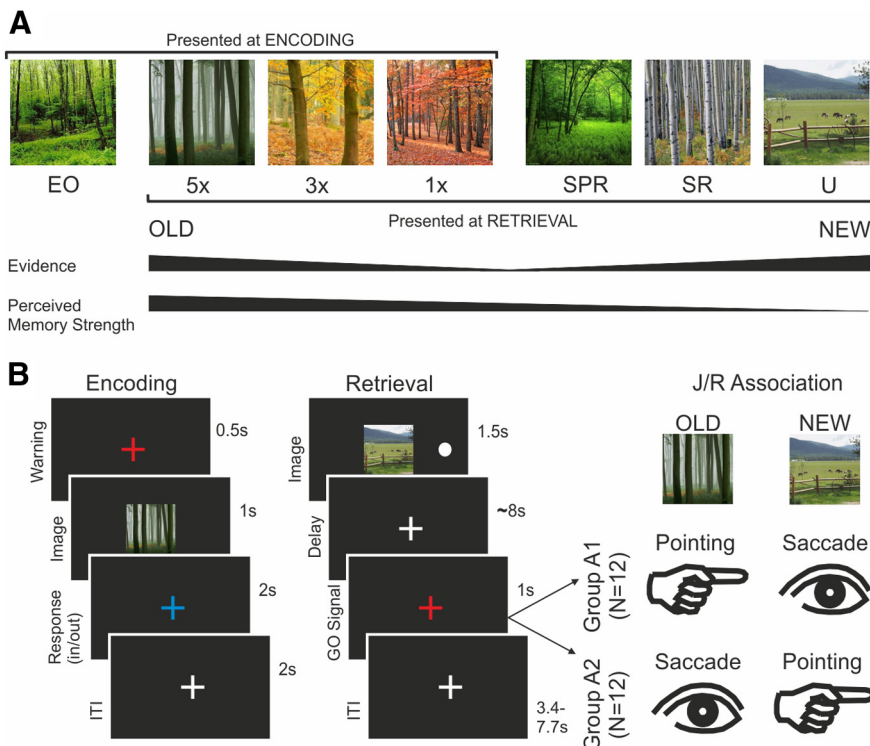
Figure 1. Experimental paradigm. **A**, Example of the visual stimuli used in the psychophysical and the fMRI experiments. In the encoding session, four images for each of 30 indoor and 30 outdoor ("forest" in the example) categories were presented at different frequencies to manipulate encoding strength. EO images were only presented at encoding. At retrieval, old (encoded) images were characterized by increasing levels of evidence (1× <3× <5×) toward old responses. Similarly, there were three types of new images. SR and SPR images were selected from the same categories ("forest" in the example) used in the encoding session: SR images were only semantically related to old images, whereas SPR images were also physically similar to EO images. Finally, U images were chosen from 60 new categories ("countryside" in the example). The manipulation of similarity between old and new images created three levels of increasing evidence toward new responses (SPR < SR < U). Perceived memory strength was supposed to be strongest for 5× old images and weakest for U images. **B**, fMRI paradigm. Left, Trial structure of the encoding task (fMRI experiment). A warning red fixation cross preceded image onset. Image was presented for 1 s, followed by fixation. Participants provided indoor/outdoor judgments. Right, Trial structure of the retrieval task. An image was presented for 1.5 s along with a left or right peripheral target (white circle). An ∼8 s delay preceded the go-signal for the execution of either a saccade or a pointing movement toward the remembered peripheral target based on the old/new judgment. The association between memory judgment and response effector (J/R association) was counterbalanced across groups (N = 12 each).

to carry out a formal model comparison between the behavioral and the fMRI data, the use of a delay paradigm for memory decisions (which prevented the use of DDM to fit behavioral data) reflected a precise intention to avoid important confounds (e.g., time-on-task) associated with evidence accumulation signals in fMRI reaction time paradigms (Ho et al., 2009; Kayser et al., 2010; Tosoni et al., 2014).

Encoding. Participants performed the session inside a mock scanner using a projector to minimize differences in stimulus presentation across sessions. The background was always black, and the fixation cross during the ITI was white. The physical similarity between EO images and SPR images was quantitatively assessed through the calculation of the RGB color correlation between image pairs within each of the 60 stimulus categories. Briefly, the 5 d (R × G × B × XCoord × YCoord) matrices of image intensity values were converted to vectors and then correlated with one another. This test was conducted to verify that images of the EO/SPR pair from one stimulus category were more similar compared with all the other possible image pairs from the same category. A one-way ANOVA with image pair as factor (15 levels) on the Fisher-transformed correlation of RGB values between corresponding voxels in each image demonstrated a significant effect of image pair ($F_{(14,826)} = 4.9$; $p < 0.0001$). Duncan *post hoc* tests showed that SPR and EO images had higher levels of RGB correlation (mean r across categories = 0.34) compared with all other possible pairs (range of mean $r = 0.11$–0.19; $p < 0.0001$), whereas no significant difference was observed in all the other possible pairs.

Retrieval. At the beginning of each run, subjects were required to hold down a button and maintain central fixation. Each trial started with the simultaneous presentation for 1.5 s of the image, covering 6° of visual angle at the center of the screen, and the peripheral target (white circle of 1° diameter) for the subsequent movement, randomly located on the left or on the right at 5.5° from fixation. A white fixation cross followed the stimulus offset until a red cross appeared, indicating the go-signal. Depending on the J/R association (group A1, A2) that was provided at the beginning of the experiment, participants were required to either release the button and rotate their wrist (without moving the shoulder or the arm) in the direction of the target while keeping central fixation (pointing response), or to move the eyes in the direction of the target direction while continuing to hold the button (saccade response), and then immediately return back to the starting point. A variable inter stimulus interval with a white fixation cross (2,3,4 MR frames) was interposed between the go-signal onset and the beginning of the next trial. Participants performed a total of 360 trials divided in 12 runs. A practice block was performed at the beginning of the experiment to ensure that participants understood the instructions, correctly executed the movements, and could perform the task above chance. Pointing response times corresponded to the release times on the button box while correct execution of movements was online monitored from the control room.

changes to test effector specificity and adapt the task to the fMRI environment. Changes mainly pertained to the retrieval sessions and were based on the same rationale used in a previous study on perceptual decision-making (Tosoni et al., 2008). First, subjects had to delay their decisions until the onset of a go-signal for action execution. A delay of 5 MR frames (∼9.57 s) was interposed between the image onset and the go-signal to temporally separate the BOLD response associated with the decision phase from activity associated with the motor execution phase. Second, a peripheral target was presented simultaneously with the image at the beginning of the trial, and subjects were instructed to report old/new judgments by executing a pointing or a saccadic eye movement toward the remembered location of that target. Third, the memory judgment/response (J/R) association was manipulated between groups, so that old judgments were associated with a pointing movement in the first and with a saccadic eye movement in the second group. The flip of the J/R association aimed at separating neural signals associated with movement selectivity from those associated with evidence modulation.

Differences in the design between the fMRI and behavioral experiment have important implications for data analysis and data comparison. Whereas the DDM was used to fit the psychophysical data (testing the effect of the experimental manipulation of memory evidence on specific parameters of the DDM), the fMRI experiment tested alternative neural implementations of the drift rate modulation observed at the behavioral level, combining evidence manipulation with a delay paradigm. Although we acknowledge that this experimental procedure did not allow

Localizer scans

Localizer scans aimed at identifying effector-specific frontoparietal regions that selectively respond to the preparation and execution of either saccadic-eye or hand-pointing movements. In a blocked fMRI design, observers alternated 18 s blocks of delayed hand pointing or saccadic eye

movements with blocks of visual fixation of variable duration (mean duration = 13 s). Each block started with a written instruction (FIX, EYE, HAND) and contained 4 trials. Each trial began with observers maintaining central fixation while holding down a button of a response pad. On each trial, a peripheral target indicating the direction of the upcoming movement appeared for 300 ms in one of 4 radial locations (1/4, 3/4, 5/4, 7/4 π) at an eccentricity of 8° of visual angle. The target was a filled white circle of 0.9° diameter. After a variable delay (1.5, 2.5, 3.5, or 4.5 s), the fixation point turned red and participants were instructed to either release the button and rotate their wrist (without moving the shoulder or the arm) in the direction of the target while keeping central fixation (pointing blocks) or move the eyes in the direction of the target while continuing to hold the button (saccade blocks), and then immediately return back to the starting point. Two runs were collected in each subject, each including 8 blocks of pointing and saccadic eye movements. Visual stimuli were displayed using an in-house toolbox running in MATLAB (MathWorks).

Behavioral data analysis
Psychophysical experiment. To test whether the manipulation of encoding strength and image relatedness effectively induced a modulation of the drift rate of evidence accumulation, we fitted the Ratcliff diffusion model (Ratcliff and McKoon, 2008) to behavioral data using the Diffusion Model Analysis Toolbox (Vandekerckhove and Tuerlinckx, 2008). To reliably select a unique model parameterization that best fitted the data, we first pooled the behavioral data across all subjects and compared the fit of several model parameterizations (Philiastides et al., 2011). This procedure ensured the selection of the best model parameterization to be used for individual fit, as the quality of fit increases with increasing number of observations (Cohen et al., 2008). Sixteen model parameterizations were compared: all the possible combination of increasing size of four parameters [drift rate (v), boundary separation (a), starting point (z), and nondecision time (Ter)], a model in which all parameters were fixed, and one in which all parameters were allowed to freely vary across conditions. Outliers were removed with a combination of two methods: data were preprocessed with an exponentially weighted moving average control method for the removal of suspected fast guesses and then a mixture model was fitted to the data to identify other contaminants of response times (Vandekerckhove and Tuerlinckx, 2007). Goodness of fit and model selection were performed using the Bayesian Information Criterion (BIC) to account for model complexity. Once the best model parameterization was determined at the group level, it was used to fit each individual subject data. Finally, significant variation of the drift rate across experimental conditions was assessed through a two-way ANOVA with Memory Status (MS: old, new) and Evidence (E: high, middle, low) as factors.

fMRI experiment. The introduction of a temporal delay between image presentation and action execution prevented from analyzing behavioral data of the recognition task using sequential sampling models. We therefore analyzed performance in terms of standard measures of accuracy.

fMRI methods
Image acquisition. Functional T2*-weighted images were collected on a Philips Achieva 3T scanner, using a gradient-echo EPI sequence to measure the BOLD contrast over the whole brain (TR = 1914 ms, TE = 25 ms, 39 slices acquired in ascending interleaved order, voxel size = 3.59 × 3.59 × 3.59 mm, 64 × 64 matrix, flip angle = 80°). Nine subjects performed the localizer scans with slightly different parameters (TR = 1869). Structural images were collected using a sagittal M-PRAGE T1-weighted sequence (TR = 8.14 ms, TE = 3.7 ms, flip angle = 8°, voxel size = 1 × 1 × 1 mm) and a T2-weighted sequence (TR = 3 s, TE = 80 ms, flip angle = 90°, voxel size = 0.98 × 1 × 1 mm, 39 slices). The fMRI runs of the point/saccade localizer and the memory task included 283 and 248 volumes/images, respectively. Preprocessing and data analysis were performed using in-house software (fIDL) developed at Washington University (St. Louis).

Preprocessing. BOLD images were motion-corrected within and between runs, corrected for across-slice timing differences, resampled into 3 mm isotropic voxels, and warped into 711–2C space, a standardized

atlas space (Talairach and Tournoux, 1988; Van Essen, 2005). Preprocessing included a whole-brain normalization correcting for changes in overall image intensity between BOLD runs.

fMRI data analysis
Localizer scans. Hemodynamic responses associated with localizers blocks were generated by convolving a function representing the duration of the process (rectangle function) with a standard hemodynamic response function (Boynton et al., 1996). Effector-selective regions were identified from single-subject z-maps of contrasts from the localizer scans as the intersection of the two statistical parametric maps resulting from the contrasts between pointing (saccades) versus saccades (pointing), and between pointing (saccades) versus fixation, thresholded at $z > 1$ and $z > 2$, respectively. Regions of interest (ROIs) were created using a peak-search algorithm that identified peaks in the uncorrected z-map and consolidated foci closer than 16 mm by coordinate averaging. Spherical ROIs of 10 mm radius were formed. These ROIs were used for independent time course analysis during the memory experiment. For display purposes, volumes were mapped to surface-based representations using the PALS atlas and CARET software (Van Essen, 2005).

Frame-by-frame model of the retrieval task. Hemodynamic responses were estimated by making no assumption about the shape of the hemodynamic response function (HRF). This frame-by-frame model provided an unbiased estimate of the time course for each trial type (Ollinger et al., 2001), generating separate delta-function regressors for each of the 14 MR frames after image onset. Hence, compared with models that assume a shape of the HRF, the present approach allowed to identify the time point in which two or multiple conditions diverged. Moreover, the use of time course analyses allowed direct comparisons with BOLD activity during perceptual decisions (Tosoni et al., 2008). The GLM included 14 task regressors: correct and incorrect trials for each of the six experimental conditions (5×, 3×, 1×, SPR, SR, U, listed by increasing evidence toward new decisions) and 2 regressors for old and new trials in which the response was executed before the go-signal (error trials). The model included terms on each scan for an intercept, linear trend, and temporal high-pass filter with a cutoff frequency of 0.009 Hz. Time courses were divided in two phases decision (frames 1–7) and execution phase (frames 8–14), both characterized by a distinct peak of BOLD activity. The decision phase included one frame after the presentation of the go-signal because this time point should not be contaminated by activity related to movement execution due to the hemodynamic delay of the BOLD response.

Voxelwise t tests. To identify cortical regions exhibiting BOLD modulations compatible with the accumulation of memory evidence independent of the J/R association, we searched for two patterns over the whole brain: (1) a monotonic BOLD response profile tracking the amount of evidence toward one of the two possible decisions (either old or new); and (2) a nonmonotonic (U-shaped) response profile tracking recognition accuracy, thus reflecting the amount of evidence regardless of the memory status of the item. To identify regions showing the former pattern, we conducted a one-sample t test across subjects (N = 24) that compared the BOLD response for the six conditions (5×, 3×, 1×, SPR, SR, U). Importantly, the t test was performed on the monotonic response magnitudes computed only over the first seven time points, corresponding to the decision phase, and conditions (correct trials only) were weighted based on the subject-specific level of "perceived memory strength," defined as the number of old responses divided by the total number of responses associated with each experimental condition. This way old 5× and new U trials were associated with strongest and weakest weights, respectively. Several features of the current approach must be emphasized. First, differently from previous analyses of "perceived oldness" (Wheeler and Buckner, 2003; Kahn et al., 2004), the present analysis was performed using correct rejections rather than false alarms for new responses. In addition, subject-specific (demeaned) behavioral measures were used to weight the BOLD responses, thus taking individual behavioral variability into account to increase the match between the behavioral and the neural responses. Finally, instead of assuming a shape of the HRF, a voxel-specific contrast function was created representing the average time course of the BOLD response to the six conditions. In

the resulting z-map, positive and negative values indicate voxels tracking evidence toward old and new decisions, respectively.

To identify regions showing a nonmonotonic response profile, the subject-specific weight associated with each condition reflected the corresponding level of recognition accuracy, so that stronger weights were assigned to easier conditions (old 5×, new U), characterized by higher evidence. In the resulting z-map, positive values indicate voxels in which BOLD activity positively scaled with the amount of evidence (easier > more difficult), whereas negative values indicate regions where activity negatively scaled with the amount of evidence (more difficult > easier). All voxelwise maps were corrected for multiple comparisons using a region size/z-score criterion combination determined by Monte-Carlo simulations, so that the resulting probability that the null hypothesis is falsely rejected anywhere in the brain is 0.05. Following standard procedure in our laboratory, we used a z-score/region size criterion corresponding to z-score = 3 and 17 contiguous face-connected voxels. Time courses were extracted for display purposes in spherical ROIs of 10 mm radius formed using a peak-search algorithm that identified peaks in the corrected z-map and consolidated foci closer than 16 mm by coordinate averaging.

Effector-selective ROI analysis. Regional time courses for each condition were estimated by averaging across all the voxels in each ROI from the localizer session. Group analyses were conducted using random-effects ANOVAs on individual time-points of the estimated hemodynamic response. For each trial phase (decision, execution), a mixed-effect ANOVA was conducted on correct trials with Memory Status (MS: old, new), Evidence (E: high, middle, low), and Time (T: 7 frames) as the within-subject factors and J/R Association (J/R: A1, A2) as the between-subjects factor. *Post hoc* analyses were performed using Duncan *post hoc* tests.

Voxelwise ANOVAs. The same ANOVA design was also conducted at the voxelwise level. Time courses were spatially smoothed before entering the ANOVA using a Gaussian filter with a FWHM of 6 mm. ANOVAs were corrected for nonindependence of time points by adjusting the degrees of freedom and for multiple comparisons using joint z-score/cluster size thresholds corresponding to z = 3.0 and a cluster size of 13 face-contiguous voxels (corresponding to $p < 0.05$, corrected).

Additional ROI analysis in regions modulated by perceived memory strength. Two additional regional ANOVAs were conducted on the decision-related time courses extracted from regions that were modulated by perceived memory strength and recognition accuracy. The first three-way ANOVA [E (5×, 3×, 1×, SPR, SR, U) by J/R association (A1, A2) by Time (7 frames)] tested whether activity for perceived memory strength was modulated by the particular effector used to report the decision (i.e., J/R association). The second three-way ANOVA [MS (old, new) by E (high, middle, low) by Time (7 frames)] tested whether evidence modulation differed across old (5×, 3×, 1×) and new items (SPR, SR, U). Importantly, when the latter analysis was conducted in regions tracking perceived memory strength, evidence levels were reversed for new items so that high evidence old trials corresponded to low evidence new trials and vice versa.

Additional HRF-assumed model. To test the consistency of the results across different analysis methods, we reanalyzed the same set of data using a standard HRF-assumed GLM approach. The model separated decision and execution phases and included 12 decision regressors [MS (old, new) × E (high, middle, low) × Accuracy (correct, incorrect)], starting at image onset, and 4 execution regressors [Movement (saccade, pointing) × Accuracy (correct, incorrect)], starting at the go-signal onset. The assumed response for each process was generated by convolving a rectangle function representing the duration of the process (1.5 s for the decision phase corresponding to image presentation time, 1 s for execution phase corresponding to go-signal duration) with a standard hemodynamic response function (Boynton et al., 1996). Voxelwise t tests were conducted using magnitudes corresponding to the decision phase.

Eye movement recording and data analysis

During the fMRI retrieval task, to ensure that subjects maintained accurate fixation during the delay period and only executed saccades when not releasing the button (and vice versa) after the go-signal, eye position

was recorded at 120 Hz through an infrared eye-tracking system (ISCAN ETL-400). Eye-movement analysis was conducted on participants with sufficient data quality in at least half of the experimental runs ($N = 10$, 5 subjects for each J/R association, 8 reliable runs per subject on average). Data were first corrected for eye-blinks, linear drift, and other sources of artifacts, such as high-frequency noise. For each trial, we then estimated a time course of eye position in the horizontal axis time-locked to trial onset (image presentation). The eye position in the 200 ms before each trial onset was used to determine the relative change in eye position during 46 consecutive time bins (250 ms each) spanning ~11.5 s after image onset (from image onset to 1 s after ITI onset). Trials were sorted based on accuracy, peripheral target location, and presence of the button release indicating a pointing response. Trials were averaged in each subject, then a grand average across subjects was computed in each bin for four conditions of interest: correct left and right pointing and saccade responses. Time courses were divided into three phases corresponding to image presentation, delay, and response.

Head movement analysis

To compare head motion across trials in which subjects executed a saccade or a pointing movement, we conducted a time-window analysis assigning MR frames to different trial types (saccade, pointing). For each trial, 7 consecutive MR frames were considered, starting at the onset of image presentation. Instantaneous head motion (framewise displacement, FD) (Power et al., 2012) was calculated using the following formula: $FDi = |\Delta dix| + |\Delta diy| + |\Delta diz| + |\Delta \alpha i| + |\Delta \beta i| + |\Delta \gamma i|$, where x, y, and z were the three translations, α, β, and γ the three rotations, and $\Delta di = d(I - 1) - di$. Rotational displacements were converted from degrees to millimeters by calculating displacement on the surface of a sphere of 50 mm radius. Differences between trial types were assessed through a two-tailed paired t tests.

Results
Behavior
Psychophysical experiment

A two-way ANOVA with Memory Status (MS: old, new) and Evidence (E: high, middle, low) as factors was conducted on reaction times and accuracy of item recognition (Fig. 2A,B). Results indicated a significant effect of Evidence [reaction times: $F_{(2,28)} = 29.2$; $p < 0.0001$; accuracy: $F_{(2,28)} = 290.8$, $p < 0.0001$] and a significant Evidence by Memory Status interaction [reaction times: $F_{(2,28)} = 5.1$; $p < 0.05$; accuracy: $F_{(2,28)} = 5.9$, $p < 0.01$]. *Post hoc* comparisons (Duncan *post hoc* tests) revealed that, although the modulation of memory evidence induced a robust parametric effect for both judgments, there was a significant old–new difference in the lowest ($p < 0.0001$) and highest ($p < 0.001$) evidence conditions. As shown in Figure 2C, which illustrates the percentage of old responses against decreasing evidence toward old decisions (perceived memory strength), old responses dropped almost linearly from ~80% (old, high evidence) to ~5% (new, high evidence). Next, we tested whether the manipulation had a specific effect on evidence accumulation, which corresponds to the drift rate parameter of the drift diffusion models (Ratcliff and McKoon, 2008). The best model parameterization at the meta-subject level according to the BIC was a model in which the drift rate was allowed to freely vary across conditions while the other parameters remained constant (Table 1). The two-way ANOVA with MS (old/new) and E (low, middle, high) on the estimates of the drift rates obtained from individual subject fitting revealed a significant effect of Evidence ($F_{(2,28)} = 17,5$; $p < 0.0001$). Thus, in accordance with our predictions, the present manipulation specifically affected the process of evidence accumulation.
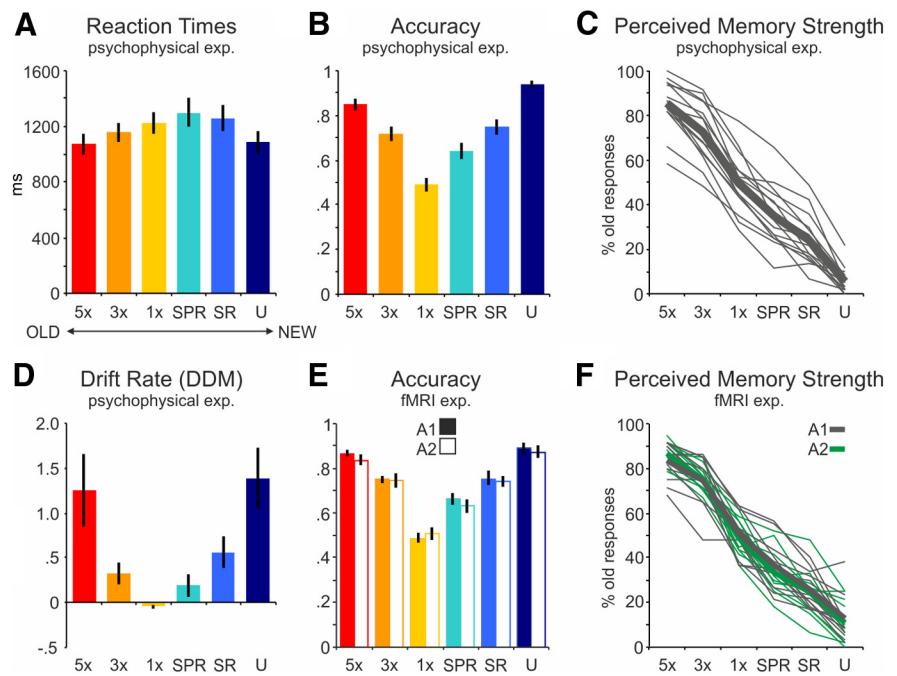
fMRI experiment

First, we tested whether the manipulation of memory evidence had a robust effect on recognition accuracy as it did in the psy-

chophysical experiment (Fig. 2E). A three-way ANOVA with MS (old, new), E (high, middle, low), and J/R (A1, A2) as factors revealed a significant main effect of E ($F_{(2,44)} = 275.0$, $p < 0.0001$) and MS ($F_{(1,22)} = 6.7$, $p < 0.05$) and a MSxE interaction effect ($F_{(2,44)} = 20.0$, $p < 0.0001$). *Post hoc* tests indicated that, similarly to the psychophysical experiment, subjects performed better at new versus old items at the lowest level of evidence (1× vs SPR, $p < 0.0001$). Importantly, there was a significant difference across the three levels of evidence for both old and new trials ($p < 0.0001$). Furthermore, the two groups had comparable performance, as no interactions were observed between J/R and E ($F_{(2,44)} = 0.2$; $p = $ not significant) or MS ($F_{(1,22)} = 0.1$; $p = $ not significant). The similarity of performance across individuals and groups can be observed also in the plot displaying perceived memory strength as a function of evidence (Fig. 2F). Overall, performance was comparable across paradigms (compare Fig. 2B,C with Fig. 2E,F).

fMRI

Voxelwise analysis: modulations tracking perceived memory strength

As a first step, we focused on the identification of signals compatible with the accumulation of memory evidence, but independent of the response effector, across the whole brain. The first analysis tested the presence of voxels where BOLD activity during the decision phase was parametrically modulated by perceived memory strength (Fig. 2F). This analysis aimed at identifying cortical regions showing a monotonic response tracking the amount of evidence toward old (older > newer, positive values) or new decisions (newer > older, negative values) in both groups. As shown in Figure 3A, B, this contrast revealed a set of regions showing a positive parametric modulation for perceived memory strength (for regions list, see Table 2), whereas no region showed the reversed pattern (i.e., tracked novelty). Figure 3C illustrates the pattern of activity from the largest cluster located in the left middle intraparietal sulcus (middle IPS). As expected, the time courses showed two distinct peaks of BOLD activity corresponding to the decision and the execution phases. Importantly, whereas the second peak (execution) showed no modulation of decision evidence, the first peak (decision) increased parametrically as a function of perceived oldness, regardless of the J/R association. The independence of the observed modulation from the particular effector used to report the decision was confirmed by a regional three-way ANOVA with E (5×, 3×, 1×, SPR, SR, U), J/R (A1, A2), and Time (7 MR frames) as factors, which revealed no significant three-way ($F_{(30,660)} = 1.18$; $p = $ not significant) and ExJ/R ($F_{(5,110)} = 0.98$; $p = $ not significant) interactions. Interestingly, as shown by a significant MSxExT interaction ($F_{(12,276)} = 2.42$; $p < 0.01$), the middle IPS showed a greater evidence modulation for old compared with new items (for details of the regional ANOVA, see Materials and Methods). Other regions tracking

Figure 2. Behavioral results. ***A–D***, Behavioral data from the psychophysical experiment. ***A***, Recognition times for the six experimental conditions. Old images are shown in warm colors, from red (5×, high evidence) to yellow (1×, low evidence), whereas new images are shown in cool colors, from light (SPR, low) to dark (U, high) blue. Subjects displayed an inverse U-shape function, with faster recognition for high evidence compared with low evidence trials. Error bars indicate SEM. ***B***, Retrieval accuracy. Participants exhibited an expected U-shape function, characterized by higher accuracy for high evidence compared with low evidence trials. ***C***, Perceived memory strength, calculated as the number of old responses divided by the total number of responses. Individual subjects are represented by thin lines, the mean of 15 subjects by the thick line. An almost linear decrease from 5× old to U new items was observed. ***D***, Estimates of the drift rate across subjects for the six experimental conditions obtained by fitting in each individual the DDM parameterization that provided the best fit at the meta-subject level. In this model, only the drift rate was allowed to vary freely across conditions, whereas other parameters remained constant. ***E,F***, Behavioral data from the fMRI experiment. ***E***, Retrieval accuracy. Solid and empty bars represent the two groups with opposite J/R association (A1, A2), characterized by very similar performance. ***F***, Perceived memory strength, separately assessed for the two groups (A1 in gray, A2 in green). The thin lines indicate individual subjects; the thick line represents the mean of 15 subjects.

Table 1. Test of DDM parameterization at the meta-subject level[a]

No.	Model parameterization	BIC
1	No (all parameters fixed)	13621
2	**v**	**13005**
3	Ter	13596
4	a	13418
5	z	13042
6	v, Ter	13032
7	v, a	13035
8	v, z	13043
9	Ter, a	13306
10	Ter, z	13046
11	a, z	13197
12	v, Ter, a	13063
13	v, Ter, z	13055
14	Ter, a, z	13186
15	v, Ter, a, z	13093
16	All (v, a, Ter, n, st, z, sz)	13219

[a]The 16 DDM model parameterizations tested at the meta-subject level for the selection of the best model for individual subjects. Goodness of fit was established using the BIC, which accounts for model complexity (i.e., number of free parameters). The BIC was used to identify the best model parameterizations for individual subject model selection. v, Drift rate; Ter, nondecision time; a, boundary; z, starting point; n, variance in drift rate; st, variance in nondecision time; sz, variance in starting point.

perceived memory strength included prefrontal regions, located in the middle frontal gyrus (MFG) just anterior to the precentral sulcus and in the inferior frontal gyrus (IFG), and the striatum, especially in the caudate nuclei (for location and results of the
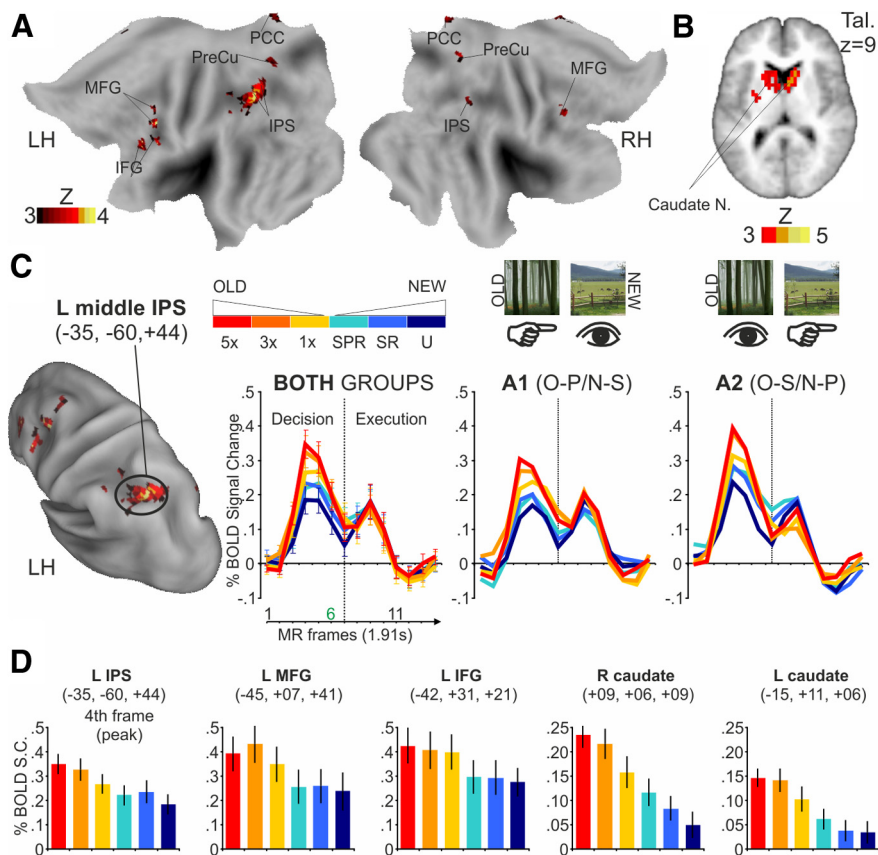
Figure 3. Perceived memory strength. *A*, The voxelwise map was obtained with a one-sample *t* test against the baseline on the magnitude of BOLD signal from the decision phase, in which a specific weight was associated to each of the six conditions based on the corresponding individual level of perceived memory strength. The map is superimposed on a flat representation of the PALS atlas (Caret software) (Van Essen, 2005). *B*, Transversal slice showing the positive response in the striatum. *C*, The left IPS shows a monotonic response tracking perceived memory strength regardless of the particular J/R association. Location on an inflated PALS representation and time courses of BOLD activity from the IPS region. Time courses of the BOLD signal change compared with baseline for the 14 MR frames after image onset are displayed for the whole group of 24 subjects and separately from subgroups with different J/R associations. The same color code of the behavioral results was used, in which response to correctly recognized old and new items is represented by warm and cool colors, respectively. The vertical dotted line in the middle of each graph separates the decision from the execution phase. Error bars indicate SEM. *D*, Percent BOLD signal change corresponding to the peak of the decision phase (fourth MR frame) from the IPS region and from other regions of the prefrontal cortex and the striatum that were modulated by perceived memory strength.

regional ANOVAs, see Fig. 3*B*; Table 2). The modulation appears stronger in the left compared with the right hemisphere. Figure 3*D* illustrates the monotonic pattern observed in five representative regions by plotting the percent BOLD signal change measured at the peak of the decision phase (fourth MR frame) for the six conditions. Notably, activity in these regions cannot be explained in terms of time-on-task because the strongest activity was found for the easiest old condition. Overall, this analysis identified a set of regions, particularly the left middle IPS, whose activity is consistent with the presence of an asymmetrical mechanism for the accumulation of evidence toward old decisions.

Voxelwise analysis: modulations tracking recognition accuracy
The second analysis tested the presence of voxels in which the BOLD activity during the decision phase was parametrically modulated by recognition accuracy. Therefore, this approach aimed at identifying cortical regions showing a nonmonotonic BOLD response (U-shaped) that tracked the amount of evidence regardless of memory status and motor response. On the basis of previous results obtained with a similar delay paradigm (Tosoni

et al., 2008), we predicted that regions involved in evidence accumulation should exhibit greater BOLD response for easier (i.e., higher evidence) compared with more difficult (i.e., lower evidence) trials. As shown in Figure 4*A*, only three regions (Fig. 4*A*, red clusters; Table 3), including the left angular gyrus (AG), the superior frontal gyrus (SFG), and the right superior temporal sulcus (STS), exhibited higher activity for easier conditions. However, as displayed in Figure 4*B*, which shows a plot of the percent BOLD signal change in left SFG and left AG at the peak of the decision phase (fourth MR frame) for the six experimental conditions, these regions exhibited a general BOLD deactivation compared with the baseline, characterized by less deactivation for easier trials. Interestingly, the location of these regions is consistent with the topography of the so-called default mode network (DMN), a set of regions that is commonly deactivated during externally oriented tasks compared with the resting state (Shulman et al., 1997; Raichle et al., 2001). In addition to this pattern of deactivation, a few regions (Table 3), including the dorsal anterior cingulate cortex (dACC), the presupplementary motor area (pre-SMA) and the anterior insula (aINS), exhibited greater positive BOLD activity for more difficult trials (for an estimate of the peak of decision activity, see Fig. 4*C*), a pattern compatible with a time-on-task effect rather than with evidence accumulation. Overall, this analysis showed that no region showed a positive BOLD activation simultaneously with an increasing BOLD response as a function of memory evidence, as predicted by a symmetrical mechanism of evidence accumulation.

HRF-assumed GLM
To test the consistency across different data analysis approaches, we repeated the same voxelwise *t* tests using a HRF-assumed GLM (see Materials and Methods). In general, the results showed that the HRF-assumed GLM was more sensitive than the frame-by-frame GLM, with almost all the regions identified with the latter included in the larger clusters obtained with the former (Fig. 5*A*,*B*). However, the analysis performed with the HRF-assumed model also identified an additional cluster in the left hippocampus (Fig. 5*C–E*) exhibiting a positive modulation by recognition accuracy (i.e., increasing BOLD response as a function of memory evidence) and a BOLD response above the baseline. Therefore, unlike regions of the DMN showing a general BOLD deactivation pattern, the left hippocampus showed a profile of activity that was undoubtedly compatible with a symmetrical mechanism of evidence accumulation.

Identification of effector-specific ROIs
To test whether key variables for memory decision-making (i.e., amount of evidence) are encoded within regions that are

**Table 2. Brain regions modulated by perceived memory strength[a]**

| No. | Hemisphere | Region | Talairach coordinates | | | z-score | No. of voxels | Regional ANOVAs | |
			x	y	z			ExJ/RxT (p)	MSxExT (p)
1	L	Caudate nucleus	−8	−1	16	4.46	92	NS	NS
2	R	Brainstem	3	−17	−8	4.30	48	NS	NS
3	L	Putamen	−24	−12	12	4.12	32	<0.01	NS
4	L	Middle frontal gyrus	−45	7	41	4.10	39	NS	NS
5	R	Caudate nucleus	9	6	9	4.00	92	NS	NS
6	L	Cuneus	−17	−84	−7	3.95	24	<0.05	NS
7	L	Inferior frontal gyrus	−42	31	21	3.90	38	NS	NS
8	L	Intraparietal sulcus	−35	−60	44	3.89	75	NS	<0.01
9	R	Cerebellum	7	−59	−36	3.82	37	NS	NS
10	L	Inferior frontal gyrus	−46	12	25	3.80	17	NS	NS
11	L	Brainstem	−3	−32	−17	3.60	44	NS	NS
12	L	Caudate nucleus	−15	11	6	3.56	67	NS	NS
13	R	Intraparietal sulcus	38	−55	49	3.48	25	NS	<0.01
14	L/R	Posterior cingulate	−2	−33	26	3.47	42	<0.01	NS
15	R	Middle frontal gyrus	40	15	45	3.40	21	NS	NS
16	L	Middle frontal gyrus	−32	7	60	3.39	28	NS	NS
17	L/R	Precuneus	−1	−72	41	3.31	29	NS	<0.01
18	L	Postcentral sulcus	−43	−42	46	3.28	17	NS	NS
19	L/R	Posterior cingulate	2	−15	26	3.04	30	NS	NS

[a]The last two columns indicate the results (significance level) of the additional regional three-way ANOVAs performed in these regions (see Materials and Methods). The first ANOVA [E (5×, 3×, 1×, SPR, SR, U) × J/R Association (A1, A2) by Time (7 frames)] tested whether evidence modulation depended on the particular effector used to report the decision. The second ANOVA [MS (old, new), E (high, middle, high), and Time (7 frames)] tested whether a different modulation was observed between old and new items. NS, Not significant.

specific for the actions used to report the decision, a set of saccade- and pointing-selective ROIs were localized in each participant by contrasting blocks of memory-guided pointing versus saccadic eye movements (Tosoni et al., 2008). Pointing-selective regions included the following: (1) a region in the medial posterior parietal cortex (parietal reach region, PRR); (2) a region along the central sulcus, including parts of the precentral/postcentral gyri (sensorimotor cortex [SMC]); and (3) a region at the intersection of the superior frontal sulcus with the precentral sulcus (frontal reach region [FRR]). Saccade-selective regions included the following: (1) a region in the posterior intraparietal sulcus (pIPS) and a region in the frontal cortex located ventrally and laterally to the FRR region (frontal eye fields [FEF]). FEF could be identified in only 22/24 subjects, whereas the other regions were identified in at least one hemisphere of each individual subject. Based on their anatomical position and functional responsiveness to pointing and saccadic eye movements, PRR and pIPS regions likely correspond to the human homologs of monkey areas MIP/V6A (Snyder et al., 1997; Galletti et al., 1999) and LIP (Colby et al., 1996; Snyder et al., 1997), respectively. The location and effector selectivity of these cortical regions has been largely documented by previous studies (Sereno et al., 2001; Astafiev et al., 2003; Connolly et al., 2003; Galati et al., 2011).

Decision signals in effector-selective regions of the PPC
Based on animal (Shadlen and Newsome, 2001) and human (Tosoni et al., 2008; Donner et al., 2009; Gould et al., 2012) stud-
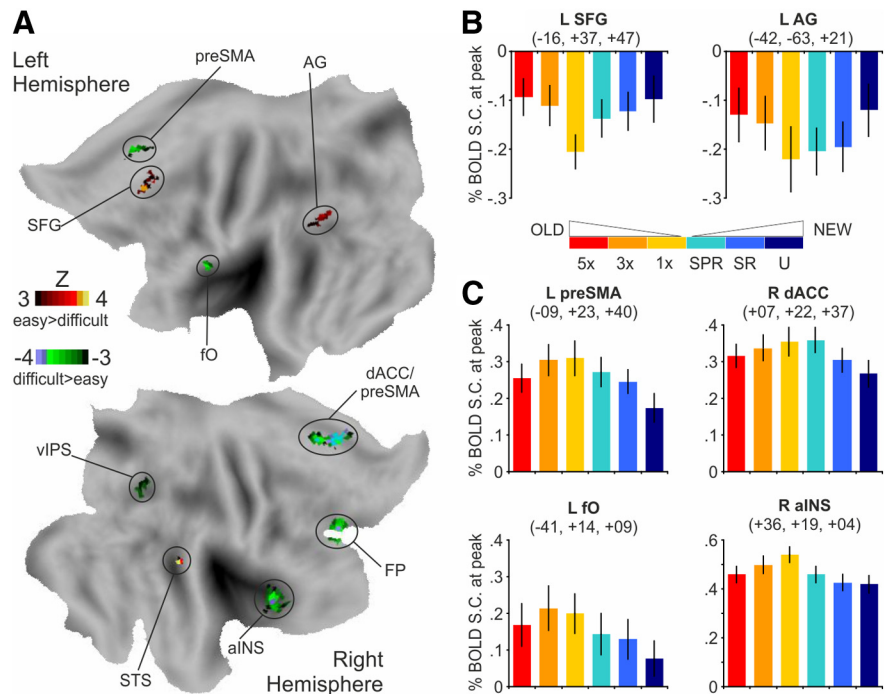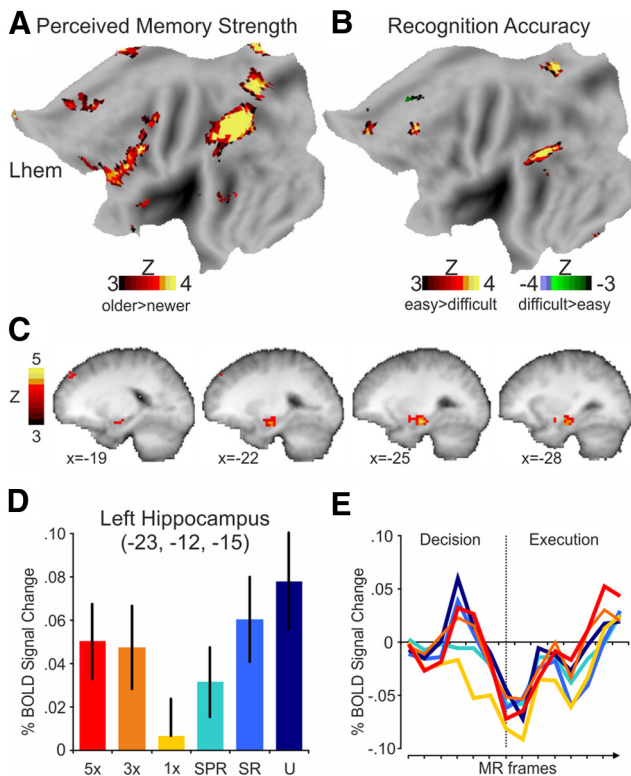

Figure 4. Recognition accuracy. **A**, Voxelwise map obtained with a one-sample t test against the baseline in which the weights for the six conditions were based on individual measures of accuracy. Colors from dark to light green indicate voxels showing higher activity for more difficult compared with easier conditions, whereas colors from red to yellow indicate voxels showing higher activity for easier compared with more difficult conditions. **B**, BOLD activity corresponding to the peak of the decision phase (fourth MR frame) from two regions where activity was greater for easier conditions (**A**, red clusters). The nonmonotonic response tracking the amount of evidence regardless of the memory status (old/new) only appeared in terms of BOLD deactivations with respect to the baseline. **C**, Peak of BOLD signal change from four regions showing greater activity for more difficult conditions.

ies supporting an intentional view of perceptual decision-making, we examined whether neural signals for memory-based decision-making are based on a similar action-based mechanism by analyzing decision signals in the effector-selective regions described above. We predicted that during the decision phase activity of parietal effector-specific regions should reflect the amount of memory evidence favoring the preferred response (Tosoni et

Table 3. Brain regions modulated by recognition accuracy[a]

| No. | Hemisphere | Region | Talairach coordinates | | | z-score | No. of voxels | Regional ANOVAs | |
			x	y	z			ExJ/RxT (p)	MSxExT (p)
Positive									
1	L	Superior frontal gyrus	−16	37	47	3.69	36	<0.01	NS
2	R	Superior temporal sulcus	52	−37	7	3.66	17	NS	NS
3	L	Angular gyrus	−42	−63	21	3.66	36	NS	NS
Negative									
4	R	Dorsal anterior cingulated	7	22	37	−4.51	48	NS	<0.05
5	R	Frontal pole	35	48	19	−3.83	32	NS	NS
6	R	Anterior insula	36	19	4	−3.81	55	NS	NS
7	L	Frontal operculum/IFG	−41	14	9	−3.56	19	NS	<0.01
8	L	Pre-SMA	−9	23	40	−3.49	26	NS	<0.05
9	R	Ventral intraparietal sulcus	25	−67	36	−3.18	17	NS	NS

[a]The last two columns indicate the results (significance level) of the additional regional three-way ANOVAs performed in these regions (see Materials and Methods). NS, Not significant.

Figure 5. Results of the HRF-assumed GLM. **A**, Voxelwise map of the regions tracking perceived memory strength superimposed on the flat PALS representation of the left hemisphere. **B**, Voxelwise map of the regions tracking recognition accuracy. **C**, Sagittal slices showing the left hippocampus cluster that positively tracked recognition accuracy. **D**, **E**, Magnitudes (left) and BOLD signal time courses (right) from the left hippocampus.

al., 2008). Because the J/R association was manipulated across subjects, this action-based hypothesis predicts an opposite modulation of memory evidence across groups.

As shown in Figure 6A, the saccade-selective pIPS region showed stronger BOLD responses for memory judgments that were associated with the preferred saccadic response (new responses for Group A1, old responses for Group A2) during both action execution and the final part of the decision delay. This result was statistically confirmed by a significant interaction of MS by J/R association during both action execution time frames (MSxJ/RxT: $F_{(6,132)} = 19.2$; $p < 0.0001$) and late frames of the decision phase (MSxJ/RxT: $F_{(6,132)} = 5.1$; $p < 0.0001$, time point 7 for group A1 ($p = 0.05$ for time point 6), time points 4–7 for group A2; $p < 0.05$, Duncan post hoc tests). Importantly inspec-

tion of the time course from the decision phase indicated that activity was not affected by the manipulation of memory evidence. This result was confirmed by the absence of a significant interaction between Evidence and any other factor of the ANOVA. Therefore, although the pIPS showed a response effector preference during the decision phase, indicating modulation by motor intention, it did not appear to encode signals related to evidence accumulation.

A different pattern of results was observed in the pointing-selective PRR region (Fig. 6B), in which an overall preference for old responses was observed in both groups during the decision phase (MSxT: $F_{(6,132)} = 6.2$; $p = 0.0001$). PRR always showed higher activity for old trials (time points 3–7 for group A1, time points 4–6 for group A2; $p < 0.05$, Duncan post hoc tests), although this result was stronger in the A1 group, in which pointing responses were associated with old decisions (MSxJ/RxT: $F_{(6,132)} = 2.4$; $p < 0.05$). Similar to the pIPS region, however, the ANOVA conducted on the decision phase revealed no significant effect of Evidence nor an interaction between Evidence and other factors. Therefore, the PRR region, which nonetheless showed a strong preference for pointing movements during the execution phase (MSxJ/RxT: $F_{(6,132)} = 14.1$; $p < 0.0001$), exhibited an overall preference for old items during the decision phase but no modulation by memory evidence. Overall, the pattern of result from the two parietal ROIs highlighted a strong segregation between signals related to evidence accumulation and movement selectivity.

Decision signals in effector-selective regions of the frontal cortex
We further assessed whether effector-specific regions of the frontal cortex exhibited signals compatible with the accumulation of memory evidence (Fig. 7). As shown in Figure 6A, the activity profile of the saccade-selective FEF region (Fig. 7A) was remarkably similar to the response observed in the pIPS. First, BOLD activity during the decision phase was higher for trials associated with a saccadic response (MSxJ/RxT: $F_{(6,120)} = 4.5$; $p < 0.0001$), but only at the end of the delay period (time points 6 and 7 for group A1, time points 5–7 for group A2; $p < 0.05$, Duncan post hoc tests). Second, no significant interaction was observed between Evidence and Time or other factors. Third, as expected, movement selectivity was present during the execution phase (MxJ/RxT: $F_{(6,108)} = 9.2$; $p < 0.0001$). A similar pattern was also observed in the pointing-selective FRR (Fig. 7B) and SMC (Fig. 7C) regions: a clear preference for trials in which the preferred response was selected at the end of the delay period (FRR: MSxJ/RxT: $F_{(6,132)} = 7.5$; $p < 0.0001$, time points 4, 6, and 7 for group A1, time points 6–7 for group A2; SMC: MS × J/R × T: $F_{(6,132)} = 10.2$; $p < 0.0001$, time points 4–7 for group A1, time points 6 and
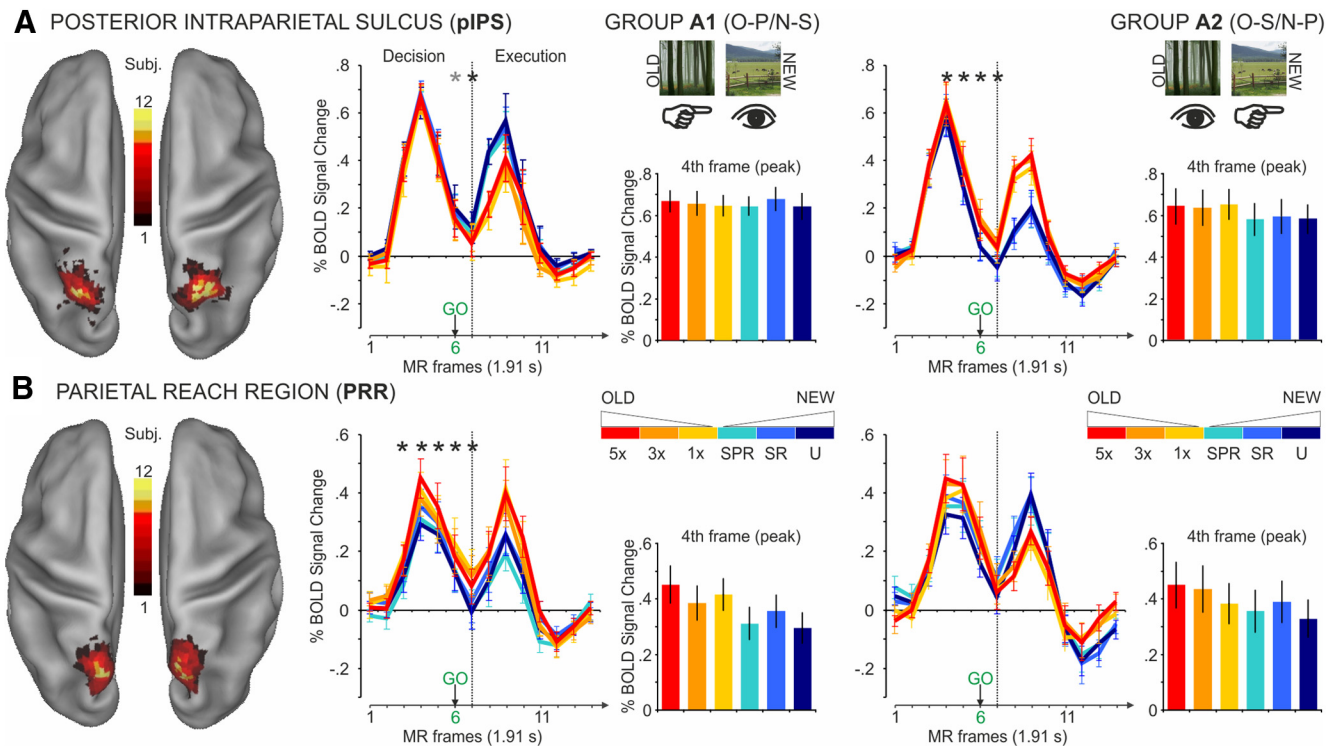
Figure 6. Parietal effector-selective regions. **A**, Anatomical location (left) and BOLD activity from the independently identified, saccade-selective pIPS region. The map on the left illustrates the degree of overlap (from red to yellow) of the ROIs identified in each participant, superimposed over an inflated cortical representation of both hemispheres. For each of two groups with opposite J/R associations, the time courses and the peak of BOLD activity in the decision phase are shown. The asterisks indicate the time point when the item associated with the preferred movement evoked greater activity compared with the nonpreferred movement: black asterisk: $p < 0.01$, gray asterisk: $p = 0.05$ (Duncan *post hoc* test relative to the MSxJ/RxT interaction of the mixed effect ANOVA). Error bars indicate SEM. **B**, Location and BOLD activity from the pointing-selective parietal reach region located in the medial PPC.

7 for group A2), no modulations by memory evidence during the decision delay and a strong selectivity for pointing movements during the execution phase (FRR: MSxJ/RxT: $F_{(6,132)} = 35.2$; $p < 0.0001$; SMC: MSxJ/RxT: $F_{(6,132)} = 88.4$; $p < 0.0001$). Overall, the analysis of decision signals on effector-selective regions of frontal cortex revealed a consistent pattern of results, with an expected selectivity for decisions associated with the preferred motor effector during response execution and the final stage of the decision phase, but no modulation related to memory evidence.

Voxelwise analysis: movement selectivity and memory evidence
To investigate whether evidence modulation coexisted with movement selectivity in other cortical regions located outside our a priori selected ROIs, a mixed-design voxelwise ANOVA was conducted across the whole cortex during the decision phase. No voxel exhibited a significant four-way interaction (MSxExJ/RxT), neither a significant three-way interaction (ExJ/RxT). Therefore, consistent with the ROI analysis, no region was found that exhibited both a preference for a particular motor effector and a modulation by the amount of memory evidence.

Eye and head movements
Mean eye position during the delay was similar across conditions, and there was no systematic bias toward the remembered target location. During image presentation (1.5 s), the mean eye position across subjects was 0.07 ± 0.61 (mean $\pm$ SD) and 0.04 ± 0.63 degrees of visual angles for left and right saccade trials, and 0.08 ± 0.68 and 0.07 ± 0.64 degrees for left and right pointing trials. During the delay period (8 s), position was 0.03 ± 0.29 (mean $\pm$ SD) and 0.00 ± 0.27 degrees for left and right saccade trials, and 0.08 ± 0.29 and 0.01 ± 0.28 degrees for left and right

pointing trials. In contrast, an expected difference was observed in the response execution period after the go-signal (1 s). Mean position was -4.94 ± 2.11 and 4.81 ± 1.87 degrees for left and right saccade trials, indicating correct eye movement execution, and -0.20 ± 0.47 and -0.11 ± 0.21 for left and right pointing trials, suggesting no systematic deviation toward target location.

The paired t test comparing the amount of head movements (FD) between saccade and pointing trials revealed no significant differences ($t_{(23)} = 0.66$; $p =$ not significant).

Discussion
Using fMRI and a novel item recognition paradigm, we investigated the neural bases of memory-based decision-making. We identified two sets of regions in which the pattern of activity was compatible with evidence accumulation, one tracking perceived memory strength and the other tracking recognition accuracy. These results suggest that item recognition decisions are supported by both asymmetrical and symmetrical accumulation mechanisms. Importantly, frontoparietal effector-specific regions were not modulated by the amount of evidence for the effector outcome, supporting a distinction between decision and motor signals.

Signals compatible with an asymmetrical accumulator
Two profiles of BOLD activity compatible with the robust behavioral modulation were tested, indicating alternative versions of the mnemonic accumulator hypothesis: asymmetrical (older > newer, or vice versa) versus symmetrical (higher > lower evidence) accumulators. The first pattern is inspired by diffusion models of episodic retrieval (Ratcliff, 1978), according to which
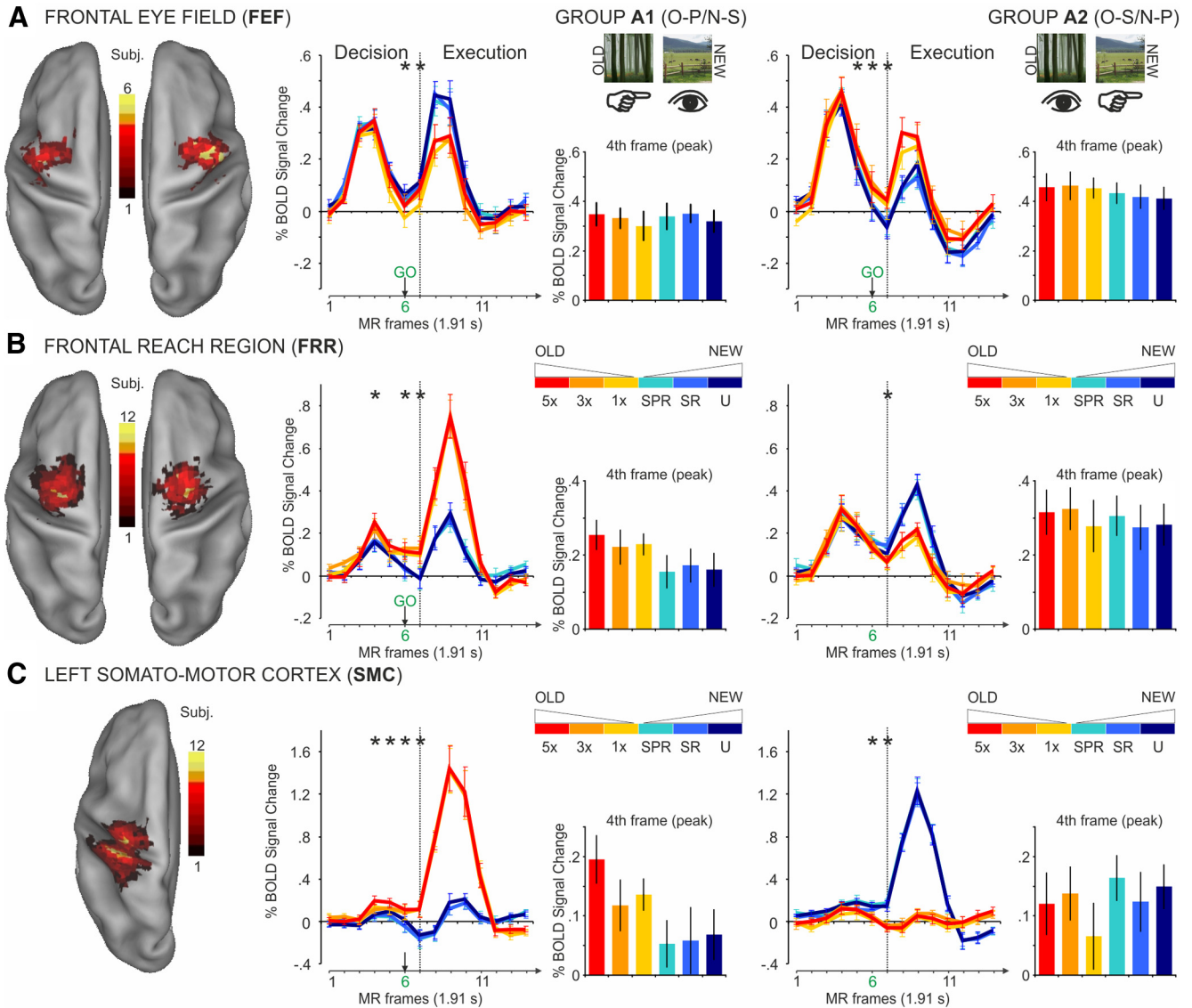
Figure 7. Frontal effector-selective regions. *A–C*, Location and BOLD activity from the independently selected, effector-specific ROI in the frontal lobe: the saccade-selective frontal eye fields (*A*) and the point selective frontal reach region (*B*) and left somatomotor cortex (*C*). Error bars indicate SEM. Asterisks indicate the time point when the item associated with the preferred movement evoked greater activity compared with nonpreferred movement.

old responses are produced when enough evidence toward relatedness (i.e., matching features between probes and items in the memory set) is accumulated, whereas new responses are returned when comparisons terminate in nonmatches. We predicted that accumulator regions should manifest a parametric modulation that tracks perceived memory strength (older > newer), although we also searched for a potential "novelty effect" (newer > older) (Huijbers et al., 2010; Jaeger et al., 2013).

We found that BOLD activity in the left middle IPS tracked the amount of evidence for old decisions, supporting the asymmetrical/old hypothesis, while no region showed a novelty effect. Although previous studies have suggested a role for the IPS in memory-based decision-making (Donaldson et al., 2010; Sestieri et al., 2011; but see Guerin and Miller, 2011), this is the first study to show a parametric modulation across six levels of evidence independent of the motor response. Moreover, the observation that evidence modulation occurs at the peak of the decision period, before movement selectivity occurs in effector-specific

regions, is compatible with a neural counter of relatedness (Donaldson et al., 2010) that feeds regions involved in later stages of the processing chain.

A similar pattern was also identified in the striatum and in lateral prefrontal cortex (IFG and MFG). The presence of retrieval-related effects in the caudate nucleus (Spaniol et al., 2009; Scimeca and Badre, 2012) has been interpreted considering the motivational significance of detecting old items, mediated by dopaminergic inputs (Han et al., 2010). Alternatively, based on its known role in movement generation and decision-making (Hikosaka et al., 2006; Ding and Gold, 2010), the striatum may represent a general convergent site for signals related to evidence accumulation, reward expectation, and action preparation, allowing flexible decision-making (Ding and Gold, 2010). Finally, the lateral prefrontal cortex has been associated with both the integration of sensory evidence during perceptual decision-making (Heekeren et al., 2008) and monitoring functions during memory retrieval (Moscovitch and Winocur, 1995), suggesting a role in high order aspects of the decision process.
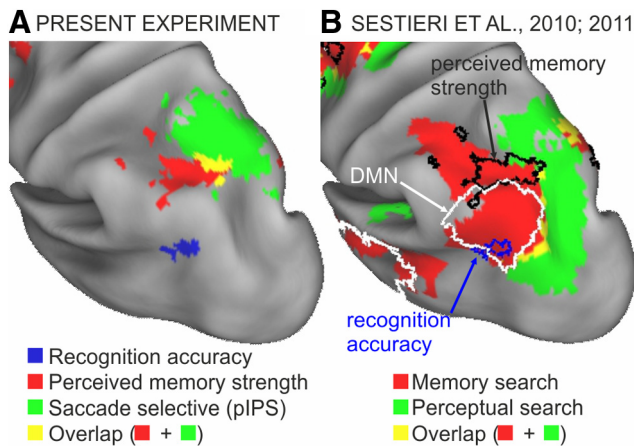
Figure 8. Topography of memory-related effects in the parietal lobe. *A*, Lateral view of the left PPC showing the spatial relationship between the regions that tracked perceived memory strength (red) and the saccade-selective region of the pIPS (green, representing the overlap of all the single subject ROIs). The figure illustrates the substantial segregation of signals related to decisions and motor intentions. The region modulated by recognition accuracy (blue) is also shown. *B*, The results of the present study were superimposed on the map of BOLD activity in response to episodic memory (red) and perceptual (green) search from a recent study from our laboratory (Sestieri et al., 2010, 2011). The figure shows that the current middle IPS region (black border) overlaps with regions involved in memory, but not perceptual, search that are located outside the DMN (white border). The spatial extent of the DMN, which includes the region modulated by recognition accuracy in the present study (blue border), was independently identified using resting state functional connectivity.

Signals compatible with a symmetrical accumulator

We also tested for a symmetrical pattern indicative of a process of evidence accumulation independent of the decision outcome (old/new). Such a mechanism would be consistent with the results of neurophysiological studies in which perceptual evidence is typically accumulated for both choices (e.g., leftward/rightward direction of motion). Notably, in contrast to previous studies using speeded responses (Ho et al., 2009; Kayser et al., 2010), the present delay paradigm predicts that symmetric accumulators manifest a positive modulation by sensory evidence (easier > more difficult) (Heekeren et al., 2006; Tosoni et al., 2008).

Among the brain regions exhibiting a U-shape pattern, the left hippocampus showed a modulation over the baseline that supports the symmetrical hypothesis. The presence of greater activity for both old and new higher evidence trials in a key memory structure such as the hippocampus is intriguing and we speculate that it may represent the fMRI correlates of the mechanisms of pattern completion and separation proposed by theoretical (Rolls, 2010) and behavioral (Duncan et al., 2012) studies. Other regions associated with the DMN (Shulman et al., 1997; Raichle et al., 2001), including the AG, showed a BOLD modulation below the baseline (weaker deactivation for easier trials), which is more difficult to interpret. If the deactivation is considered as the mere effect of an ambiguous baseline (Stark and Squire, 2001), activity in DMN regions may underlie the same symmetrical accumulation pattern observed in the hippocampus. However, it is also well known that during externally/perceptually oriented paradigms DMN regions display a load/difficulty-dependent deactivation pattern (McKiernan et al., 2003; Singh and Fawcett, 2008). Thus, BOLD response in DMN regions may mirror the pattern of BOLD modulations found in regions of the so called cingulo-opercular network (Dosenbach et al., 2006; Sestieri et al., 2014), including the dACC, pre-SMA, and aINS, who showed an inverse U-shape pattern (less positive activity for easier trials). Impor-

tantly, this latter activity profile is compatible with time-on-task effects (Grinband et al., 2008), task difficulty or the need for top-down attention, but not with evidence accumulation, at least under the present assumptions.

Segregation between decisions and motor signals

The mnemonic accumulator hypothesis derives from an explicit analogy between retrieval effects observed in human fMRI studies and the pattern of firing rate observed in monkey LIP during perceptual decisions. The discovery of evidence modulations in an oculomotor region such as the LIP provided the basis for an intentional framework (Shadlen et al., 2008), according to which decision processes are integral to sensorimotor systems. In the human brain, activity modulations consistent with the intentional account have been found in effector-specific regions of the frontoparietal cortex during perceptual decision-making (Tosoni et al., 2008; Donner et al., 2009). In contrast, here we show that BOLD modulations for memory-based decision-making are largely independent from signals related to motor intentions. Interestingly, unlike the majority of effector-specific ROIs that simply tracked the decision outcome regardless of memory evidence (compatible with action planning), the PRR always displayed a preference for old items. However, the memory effect in PRR (see also Wagner et al., 2005) did not interact with evidence modulation, confirming a functional segregation between decision and motor intentional signals.

We acknowledge that the lack of a significant effect may reflect sensitivity issues (e.g., insufficient variability in evidence values across trial bins). However, we note that the current approach was designed to be particularly sensitive to such effects. First, the manipulation of decision evidence was coupled with a direct decision-movement association. Second, the regional approach minimized Type 1 errors associated with corrections for multiple comparisons and accounted for individual anatomical variability. Finally, a sensitivity issue did not apply to other cortical regions, such as those described above.

The apparent distinction between the neural mechanisms of perceptual and memory-based decisions can have several explanations. Whereas perceptual decisions involve sensorimotor transformations, memory-based decisions are thought to require an additional feature comparison between the sensory input and the items in the memory set, which may necessitate the additional activation of stimulus- and response-independent regions. Furthermore, the two kinds of decisions involve a different relationship with the motor system. Specifically, effector-specific regions are usually defined through their sensorimotor properties (i.e., cue-target sustained activity) and have been more traditionally associated with working-memory than with long-term memory. This may explain why movement specificity in these regions has been shown to interact with the manipulation of perceptual but not memory evidence. At a more theoretical level, our results support a fundamental distinction between the selection and modulation of on-line/sensory versus off-line/mnemonic information, also based on the exclusive direct link between the former type of processing and the motor system (Sestieri et al., 2010; Chun et al., 2011).

Topography of signals for memory-based decisions in the PPC

Figure 8 displays the functional subdivision of the lateral PPC based on the three profiles of BOLD activity identified in the present study (Fig. 8A) and the pattern of BOLD modulations during memory versus perceptual search identified in our previ-

ous studies (Fig. 8B) (Sestieri et al., 2010, 2011). Whereas the middle IPS and the AG overlap with extra- and intra-DMN regions involved in memory search, respectively, the saccade-selective ROIs overlap with regions involved in perceptual search. Although the present findings advance our understanding of the functional subdivision of the lateral PPC, we acknowledge that the current study suffers from intrinsic limitations of the fMRI technique, such as poor temporal resolution and temporal summation of BOLD signal. Therefore, even if the pattern of regions tracking memory strength or recognition accuracy fits well with their role of symmetrical/asymmetrical accumulators, more work is needed to specify their temporal dynamics and their causal role in evidence accumulation.

The involvement of the middle IPS in memory-based decision-making is consistent with the idea that dorsal PPC regions are more directly involved in postretrieval than in direct retrieval processes (Vilberg and Rugg, 2008; Nelson et al., 2010), whereas it does not match the prediction of top-down attentional accounts (i.e., higher activity for more difficult items) (Cabeza et al., 2008). The functional role of ventral PPC regions is less clear. Although the positive BOLD modulation observed in our previous study (Sestieri et al., 2011) suggested a role in cued recollection (see also Johnson and Rugg, 2007), the lack of strong recollection demands (Wheeler and Buckner, 2004; Hutchinson et al., 2014) or online manipulation/maintenance of retrieved information (Sestieri et al., 2011; Vilberg and Rugg, 2012) may explain the absence of positive activity in the present study. Nonetheless, the evidence that the AG exhibits similar activity for old and new high evidence trials (U-shape function) suggests that the AG does not simply respond to recollection but also to novelty detection. Therefore, the role of the AG during item recognition appears more consistent with decision-making (see also Sestieri et al., 2013) or, alternatively, with bottom-up attentional capture (Cabeza et al., 2008).

In conclusion, the present study indicates that item recognition decisions are mediated by a combination of symmetric and asymmetric accumulation mechanisms that are independent from motor intentions.

References

Astafiev SV, Shulman GL, Stanley CM, Snyder AZ, Van Essen DC, Corbetta M (2003) Functional organization of human intraparietal and frontal cortex for attending, looking, and pointing. J Neurosci 23:4689–4699. Medline

Boynton GM, Engel SA, Glover GH, Heeger DJ (1996) Linear systems analysis of functional magnetic resonance imaging in human V1. J Neurosci 16:4207–4221. Medline

Cabeza R, Ciaramelli E, Olson IR, Moscovitch M (2008) The parietal cortex and episodic memory: an attentional account. Nat Rev Neurosci 9:613–625. CrossRef Medline

Chun MM, Golomb JD, Turk-Browne NB (2011) A taxonomy of external and internal attention. Annu Rev Psychol 62:73–101. CrossRef Medline

Cohen AL, Sanborn AN, Shiffrin RM (2008) Model evaluation using grouped or individual data. Psychon Bull Rev 15:692–712. CrossRef Medline

Colby CL, Duhamel JR, Goldberg ME (1996) Visual, presaccadic, and cognitive activation of single neurons in monkey lateral intraparietal area. J Neurophysiol 76:2841–2852. Medline

Connolly JD, Andersen RA, Goodale MA (2003) fMRI evidence for a 'parietal reach region' in the human brain. Exp Brain Res 153:140–145. CrossRef Medline

Criss AH, Wheeler ME, McClelland JL (2013) A differentiation account of recognition memory: evidence from fMRI. J Cogn Neurosci 25:421–435. CrossRef Medline

Daselaar SM, Fleck MS, Cabeza R (2006) Triple dissociation in the medial temporal lobes: recollection, familiarity, and novelty. J Neurophysiol 96:1902–1911. CrossRef Medline

Ding L, Gold JI (2010) Caudate encodes multiple computations for perceptual decisions. J Neurosci 30:15747–15759. CrossRef Medline

Donaldson DI, Wheeler ME, Petersen SE (2010) Remember the source: dissociating frontal and parietal contributions to episodic memory. J Cogn Neurosci 22:377–391. CrossRef Medline

Donner TH, Siegel M, Fries P, Engel AK (2009) Buildup of choice-predictive activity in human motor cortex during perceptual decision making. Curr Biol 19:1581–1585. CrossRef Medline

Dosenbach NU, Visscher KM, Palmer ED, Miezin FM, Wenger KK, Kang HC, Burgund ED, Grimes AL, Schlaggar BL, Petersen SE (2006) A core system for the implementation of task sets. Neuron 50:799–812. CrossRef Medline

Duncan K, Sadanand A, Davachi L (2012) Memory's penumbra: episodic memory decisions induce lingering mnemonic biases. Science 337:485–487. CrossRef Medline

Galati G, Committeri G, Pitzalis S, Pelle G, Patria F, Fattori P, Galletti C (2011) Intentional signals during saccadic and reaching delays in the human posterior parietal cortex. Eur J Neurosci 34:1871–1885. CrossRef Medline

Galletti C, Fattori P, Kutz DF, Gamberini M (1999) Brain location and visual topography of cortical area V6A in the macaque monkey. Eur J Neurosci 11:575–582. CrossRef Medline

Gold JI, Shadlen MN (2007) The neural basis of decision making. Annu Rev Neurosci 30:535–574. CrossRef Medline

Gould IC, Nobre AC, Wyart V, Rushworth MF (2012) Effects of decision variables and intraparietal stimulation on sensorimotor oscillatory activity in the human brain. J Neurosci 32:13805–13818. CrossRef Medline

Grinband J, Wager TD, Lindquist M, Ferrera VP, Hirsch J (2008) Detection of time-varying signals in event-related fMRI designs. Neuroimage 43:509–520. CrossRef Medline

Guerin SA, Miller MB (2011) Parietal cortex tracks the amount of information retrieved even when it is not the basis of a memory decision. Neuroimage 55:801–807. CrossRef Medline

Han S, Huettel SA, Raposo A, Adcock RA, Dobbins IG (2010) Functional significance of striatal responses during episodic decisions: recovery or goal attainment? J Neurosci 30:4767–4775. CrossRef Medline

Heekeren HR, Marrett S, Ruff DA, Bandettini PA, Ungerleider LG (2006) Involvement of human left dorsolateral prefrontal cortex in perceptual decision making is independent of response modality. Proc Natl Acad Sci U S A 103:10023–10028. CrossRef Medline

Heekeren HR, Marrett S, Ungerleider LG (2008) The neural systems that mediate human perceptual decision making. Nat Rev Neurosci 9:467–479. CrossRef Medline

Hikosaka O, Nakamura K, Nakahara H (2006) Basal ganglia orient eyes to reward. J Neurophysiol 95:567–584. CrossRef Medline

Ho TC, Brown S, Serences JT (2009) Domain general mechanisms of perceptual decision making in human cortex. J Neurosci 29:8675–8687. CrossRef Medline

Huijbers W, Pennartz CM, Daselaar SM (2010) Dissociating the "retrieval success" regions of the brain: effects of retrieval delay. Neuropsychologia 48:491–497. CrossRef Medline

Hutchinson JB, Uncapher MR, Weiner KS, Bressler DW, Silver MA, Preston AR, Wagner AD (2014) Functional heterogeneity in posterior parietal cortex across attention and episodic memory retrieval. Cereb Cortex 24:49–66. CrossRef Medline

Jaeger A, Konkel A, Dobbins IG (2013) Unexpected novelty and familiarity orienting responses in lateral parietal cortex during recognition judgment. Neuropsychologia 51:1061–1076. CrossRef Medline

Johnson JD, Rugg MD (2007) Recollection and the reinstatement of encoding-related cortical activity. Cereb Cortex 17:2507–2515. CrossRef Medline

Kahn I, Davachi L, Wagner AD (2004) Functional-neuroanatomic correlates of recollection: implications for models of recognition memory. J Neurosci 24:4172–4180. CrossRef Medline

Kayser AS, Buchsbaum BR, Erickson DT, D'Esposito M (2010) The functional anatomy of a perceptual decision in the human brain. J Neurophysiol 103:1179–1194. CrossRef Medline

Konkle T, Brady TF, Alvarez GA, Oliva A (2010) Scene memory is more detailed than you think: the role of categories in visual long-term memory. Psychol Sci 21:1551–1556. CrossRef Medline

McKiernan KA, Kaufman JN, Kucera-Thompson J, Binder JR (2003) A parametric manipulation of factors affecting task-induced deactivation in

functional neuroimaging. J Cogn Neurosci 15:394–408. CrossRef Medline

Moscovitch M, Winocur G (1995) Frontal lobes, memory, and aging. Ann N Y Acad Sci 769:119–150. CrossRef Medline

Nelson SM, Cohen AL, Power JD, Wig GS, Miezin FM, Wheeler ME, Velanova K, Donaldson DI, Phillips JS, Schlaggar BL, Petersen SE (2010) A parcellation scheme for human left lateral parietal cortex. Neuron 67:156–170. CrossRef Medline

Ollinger JM, Shulman GL, Corbetta M (2001) Separating processes within a trial in event-related functional MRI: I. The method. Neuroimage 13:210–217. CrossRef Medline

Philiastides MG, Auksztulewicz R, Heekeren HR, Blankenburg F (2011) Causal role of dorsolateral prefrontal cortex in human perceptual decision making. Curr Biol 21:980–983. CrossRef Medline

Power JD, Barnes KA, Snyder AZ, Schlaggar BL, Petersen SE (2012) Spurious but systematic correlations in functional connectivity MRI networks arise from subject motion. Neuroimage 59:2142–2154. CrossRef Medline

Raichle ME, MacLeod AM, Snyder AZ, Powers WJ, Gusnard DA, Shulman GL (2001) A default mode of brain function. Proc Natl Acad Sci U S A 98:676–682. CrossRef Medline

Ratcliff R (1978) A theory of memory retrieval. Psychol Rev 85:59–108. CrossRef

Ratcliff R, McKoon G (2008) The diffusion decision model: theory and data for two-choice decision tasks. Neural Comput 20:873–922. CrossRef Medline

Ratcliff R, Thapar A, McKoon G (2004) A diffusion model analysis of the effects of aging on recognition memory. J Mem Lang 50:408–424. CrossRef

Rolls ET (2010) A computational theory of episodic memory formation in the hippocampus. Behav Brain Res 215:180–196. CrossRef Medline

Scimeca JM, Badre D (2012) Striatal contributions to declarative memory retrieval. Neuron 75:380–392. CrossRef Medline

Sereno MI, Pitzalis S, Martinez A (2001) Mapping of contralateral space in retinotopic coordinates by a parietal cortical area in humans. Science 294:1350–1354. CrossRef Medline

Sestieri C, Shulman GL, Corbetta M (2010) Attention to memory and the environment: functional specialization and dynamic competition in human posterior parietal cortex J Neurosci 30:8445–8456. CrossRef

Sestieri C, Corbetta M, Romani GL, Shulman GL (2011) Episodic memory retrieval, parietal cortex, and the default mode network: functional and topographic analyses. J Neurosci 31:4407–4420. CrossRef Medline

Sestieri C, Capotosto P, Tosoni A, Romani GL, Corbetta M (2013) Interference with episodic memory retrieval following transcranial stimulation of the inferior but not the superior parietal lobule. Neuropsychologia 51:900–906. CrossRef Medline

Sestieri C, Corbetta M, Spadone S, Romani GL, Shulman GL (2014) Domain-general signals in the cingulo-opercular network for visuospatial attention and episodic memory. J Cogn Neurosci 26:551–568. CrossRef Medline

Shadlen MN, Newsome WT (2001) Neural basis of a perceptual decision in the parietal cortex (area LIP) of the rhesus monkey. J Neurophysiol 86:1916–1936. Medline

Shadlen MN, Kiani R, Hanks TD, Churchland AK (2008) Neurobiology of

decision making: an intentional framework. Cambridge, MA: Massachusetts Institute of Technology.

Shulman GL, Fiez JA, Corbetta M, Buckner RL, Miezin FM, Raichle ME, Petersen SE (1997) Common blood flow changes across visual tasks: II. Decreases in cerebral cortex. J Cogn Neurosci 9:648–663. CrossRef Medline

Singh KD, Fawcett IP (2008) Transient and linearly graded deactivation of the human default-mode network by a visual detection task. Neuroimage 41:100–112. CrossRef Medline

Smith PL, Ratcliff R (2004) Psychology and neurobiology of simple decisions. Trends Neurosci 27:161–168. CrossRef Medline

Snyder LH, Batista AP, Andersen RA (1997) Coding of intention in the posterior parietal cortex. Nature 386:167–170. CrossRef Medline

Spaniol J, Davidson PS, Kim AS, Han H, Moscovitch M, Grady CL (2009) Event-related fMRI studies of episodic encoding and retrieval: meta-analyses using activation likelihood estimation. Neuropsychologia 47:1765–1779. CrossRef Medline

Stark CE, Squire LR (2001) When zero is not zero: the problem of ambiguous baseline conditions in fMRI. Proc Natl Acad Sci U S A 98:12760–12766. CrossRef Medline

Talairach J, Tournoux P (1988) Co-planar stereotaxic atlas of the human brain. New York: Thieme Medical.

Tosoni A, Galati G, Romani GL, Corbetta M (2008) Sensory-motor mechanisms in human parietal cortex underlie arbitrary visual decisions. Nat Neurosci 11:1446–1453. CrossRef Medline

Tosoni A, Corbetta M, Committeri G, Calluso C, Pezzulo G, Romani GL, Galati G (2014) Decision and action planning signals in human posterior parietal cortex during delayed perceptual choices. Eur J Neurosci. Advance online publication. Retrieved March 11, 2014. doi: 10.1111/ejn.12511. CrossRef Medline

Van Essen DC (2005) A population-average, landmark- and surface-based (PALS) atlas of human cerebral cortex. Neuroimage 28:635–662. CrossRef Medline

Vandekerckhove J, Tuerlinckx F (2007) Fitting the Ratcliff diffusion model to experimental data. Psychon Bull Rev 14:1011–1026. CrossRef Medline

Vandekerckhove J, Tuerlinckx F (2008) Diffusion model analysis with MATLAB: a DMAT primer. Behav Res Methods 40:61–72. CrossRef Medline

Vilberg KL, Rugg MD (2008) Memory retrieval and the parietal cortex: a review of evidence from a dual-process perspective. Neuropsychologia 46:1787–1799. CrossRef Medline

Vilberg KL, Rugg MD (2012) The neural correlates of recollection: transient versus sustained fMRI effects. J Neurosci 32:15679–15687. CrossRef Medline

Wagner AD, Shannon BJ, Kahn I, Buckner RL (2005) Parietal lobe contributions to episodic memory retrieval. Trends Cogn Sci 9:445–453. CrossRef Medline

Wheeler ME, Buckner RL (2003) Functional dissociation among components of remembering: control, perceived oldness, and content. J Neurosci 23:3869–3880. Medline

Wheeler ME, Buckner RL (2004) Functional-anatomic correlates of remembering and knowing. Neuroimage 21:1337–1349. CrossRef Medline